Real-Time Simulation of Thin Rod

Min Gyu Choi[1] and Oh-young Song[2]
[1]Department of Computer Science, Kwangwoon University, Korea
[e-mail: mgchoi@kw.ac.kr]
[2]Department of Digital Contents, Sejong University, Korea
[e-mail: oysong@sejong.ac.kr]
*Corresponding author: Oh-young Song

Received November 30, 2012; revised February 4, 2013; accepted February 26, 2013; published April 30, 2013

Abstract

This paper proposes a real-time simulation technique for thin rods undergoing large rotational deformation. Rods are thin objects such as ropes and hairs that can be abstracted as one-dimensional structures. Development of a real-time physical model that can produce visually convincing animation of thin rods has been a challenging problem in computer graphics. We adopt continuum mechanics to formulate the governing equation, and develop a modal warping technique for rods to integrate the governing equation in real-time; This is a novel extension of the previous modal warping techniques developed for solids and shells. Experimental results show that the proposed method runs in real-time even for large meshes and it can simulate large bending and/or twisting deformations.

Keywords: Physics-based animation, real-time simulation, modal warping, deformation, thin rod simulation

This work was financially supported by the grant from the strategic technology development program (Project No. KI001818) of both the MKE(Ministry of Knowledge Economy) and MCST(Ministry of Culture, Sports and Tourism) of Korea and the Research Grant of Kwangwoon University in 2012. This research was also supported by Basic Science Research Program through the National Research Foundation of Korea funded by the Ministry of Education, Science and Technology (No. 2011-0012878) and the Industrial Strategic technology development program, 10041772, the Development of an Adaptive Mixed-Reality Space based on Interactive Architecture funded by the Ministry of Knowledge Economy (MKE, Korea).

http://dx.doi.org/10.3837/tiis.2013.04.014

1. Introduction

Three-dimensional flexible rod-like objects such as ropes and hairs frequently appear in computer-generated scenes. Non-zero thickness of these objects is a crucial factor in their dynamic movements. Nevertheless, they are often abstracted as one-dimensional entities, regarding the rest as visual details. In this paper, we present a physics-based real-time simulation technique for thin rods undergoing large rotational deformation.

Simulation of 3D solids has been researched extensively in computer graphics [1, 2, 3, 4, 5]. Because thin rods are special degenerate cases of 3D solids, one may apply techniques developed for 3D solids to the simulation of thin rods. Unfortunately, this approach would not produce satisfactory results; Modeling thin rods as 3D elastic solids requires very fine meshes to correctly capture the global bending and/or twisting behavior. As a consequence, it requires a large amount of computation time, and thus it cannot be used for real-time simulation.

There is a different approach to simulating thin rods, namely, employing mass-spring models [6, 7, 8]. Bending behavior can be addressed using Euler angles of adjacent edges after representing a thin rod as a serial chain, however twisting behavior cannot be handled correctly. In addition, direct integration of Euler angles incur numerical instabilities. By introducing additional edges and measuring bending deformation using stretching/shortening of the edge lengths, the mesh nodes themselves can be integrated robustly. However, twisting deformation cannot still be handled correctly. Furthermore, it is difficult to specify material constants of thin rods using mass-spring constants.

Physically-accurate simulation of elastodynamic deformation of a thin rod structure has been extensively studied [9, 10, 11]. However, accurate modeling and simulation of large deformation with a moderately-sized 1D mesh has difficulties not only in formulating the nonlinear governing equation but also in achieving real-time performance because the numerical instability caused by nonlinearity requires very small time steps of integration. Pai [12] applied the Cosserat rod model to the simulation of a strand. Bertails *et al.* [13] proposed a piecewise helical discretization to produce animations of curly hair using few elements per strand. Bergou *et al.* [14] proposed an approach that applies discrete differential geometry to physical modeling of elastic rods, which is further extended for viscous threads [15]. In this approach, rigid-coupling is required to simulate a thin rod structure with junctions.

Meanwhile, Choi and Ko [16] proposed a technique called *modal warping*, which can simulate large rotational deformation of 3D elastic solids in real-time. However, this technique is not for thin rods although it was extended to cope with shells [17]. On the other hand, Stam [18], Chang *et al.* [19], and Diener *et al.* [20] proposed modal analysis techniques that can simulate elastodynamic deformation of thin rods in real-time. However, the techniques could not be used for simulating large rotational deformation because the governing equations are obtained by assuming small deformation.

The present work is based on the continuum mechanics for thin rods and the modal warping technique; Adopting the FEM formulation for small deformation [10], we develop a novel real-time simulation framework for thin rods undergoing large rotational deformation by extending the modal warping technique [16, 17].

2. Dynamics of Thin Rods

In this section, we briefly describe the dynamics of thin rods. Detailed explanations can be found in [10]. We use a one-dimensional mesh to represent a thin rod, and formulate its dynamics with continuum mechanics and FEM. A one-dimensional rod mesh consists of three-dimensional rod elements separated by nodes. That is, an edge connecting a pair of nodes becomes a rod element for FEM. Each element has its own local coordinate frame as illustrated in **Fig. 1**. The *x*-axis is placed along the rod element, chosen in such a way that a bending moment does not produce any axial deformation. The *y*- and *z*-axes are the principal inertia axes for bending, defined in such a way that a bending moment about the *y*-axis produces no bending about the *z*-axis, and vice versa.

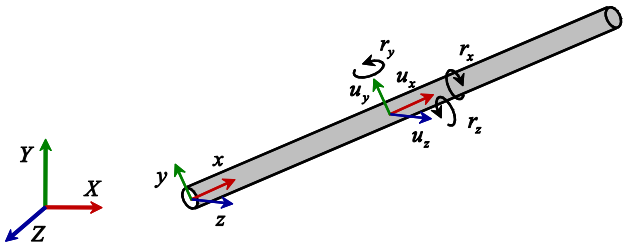

Fig. 1. Configuration of a rod element

The displacement of a material point in a rod element is obtained by interpolating the displacements of the both ends. To maintain continuity of bending in an element and across elements, we employ the cubic Hermitian shape functions for displacements along the y- and *z*-axes, and the linear shape functions for the displacement along the x-axis. Thus, a node in an element has 6 DOFs. Three are from the positional displacement (u_X , u_Y , u_Z) expressed in the local coordinate frame, and the others are from the rotational displacement (r_X , r_Y , r_Z) about each axis. Here, r_X is owing to twisting about the *x*-axis, and r_Y and r_Z are owing to bending about the *y*- and *z*-axes, respectively. When the rotational displacement is moderately small, the slope of deflection is the same with the rotation angle. Thus, the rotations r_Y and r_Z are linked to the positional displacement by

$$r_y = -\frac{du_z}{dx} \quad \text{and} \quad r_z = \frac{du_y}{dx}. \tag{1}$$

2.1 Elastic and Kinetic Energies

In the context of the kinematic Bernoulli assumptions for rods with no shear deflection, the strain energy of the rod element undergoing infinitesimal deformation can be expressed in the form:

$$U_e = \frac{1}{2}\int_0^l \left[EI_y \left(\frac{\partial r_y}{\partial x}\right)^2 + EI_z \left(\frac{\partial r_z}{\partial x}\right)^2 + GJ_x \left(\frac{\partial r_x}{\partial x}\right)^2 + EA \left(\frac{\partial u_x}{\partial x}\right)^2 \right] dx. \tag{2}$$

Here, the first two terms represent the bending energies about the *y*- and *z*-axes, respectively. The third term is for the torsional energy about the *x*-axis. The last term represents the

extension energy of the rod. E and G denote Young's modulus and the shear modulus, respectively. l is the length of the rod, and A is its cross section area . I_y and I_z are the area moments of inertia representing the bending stiffnesses about the y- and z-axes, respectively, and J_x is the polar moment of inertia representing the torsional stiffness about the x-axis. When the cross section of a rod is a disc with a radius r, $A = \pi r^2$, $I_y = I_z = \pi r^4/4$, and $J_x = \pi r^4/2$.

The kinetic energy of a rod is computed in a manner similar to the elastic energy:

$$T_e = \frac{1}{2}\int_0^l \left[\rho A\left(\dot{u}_x^2 + \dot{u}_y^2 + \dot{u}_z^2\right) + \rho J_x \dot{r}_x^2\right] dx. \tag{3}$$

The first three terms represent the translational kinetic energy and the last one describes the rotational kinetic energy about the x-axis. ρ denotes the density of the rod.

2.2 Governing Equation

Let $\mathbf{u}_e$ be the 12-dimensional vector containing the positional displacements and the rotational displacements at both ends of a rod element. Then, from Eq. (2), the discretized strain energy of the rod element can be expressed in the form:

$$U_e = \frac{1}{2}\mathbf{u}_e^T \mathbf{K}_e \mathbf{u}_e, \tag{4}$$

where $\mathbf{K}_e$ is the 12×12 stiffness matrix of the rod element defined in the local coordinate frame. The discretized kinetic energy of the rod element can be obtained from Eq. (3) in a similar manner and written in the form:

$$T_e = \frac{1}{2}\dot{\mathbf{u}}_e^T \mathbf{M}_e \dot{\mathbf{u}}_e, \tag{5}$$

where $\mathbf{M}_e$ is the 12×12 mass matrix defined in the local coordinate frame of the rod element.

To simulate a rod represented with a FEM mesh of n nodes, we need to assemble Eq. (4) and (5) in the global coordinate frame. Let $\mathbf{u}(t)$ be a $6n$-dimensional generalized displacement vector containing all the positional and rotational displacements of the n nodes transformed into the global coordinate frame. Then, the governing equation for elastodynamics deformation of the thin rod can be written in the Euler-Lagrange form [10]:

$$\mathbf{M}\ddot{\mathbf{u}} + \mathbf{C}\dot{\mathbf{u}} + \mathbf{K}\mathbf{u} = \mathbf{F}, \tag{6}$$

where $\mathbf{C} = \xi\mathbf{M} + \zeta\mathbf{K}$ is a damping matrix with Rayleigh damping constants ξ and ζ. $\mathbf{F}$ is a $6n$-dimensional vector representing the external forces acting on the n nodes of the thin rod. We note that Eq. (6) is valid only for moderately small deformation. As a consequence, when applied to the simulation of a thin rod undergoing large rotational deformation, it can be elongated unrealistically.

3. Modal Warping for Rods

For real-time simulation of thin rods, we adopt the modal warping framework [16]. Because the framework is for 3D solids, we need to modify it for thin rods. A major modification is in the way of tracking the orientation of the local coordinate frame attached to each mesh node. This modification is similar to the modification required for shells [17], but the former is more straightforward than the latter owing to the structure of the generalized displacement vector, as will be explained in Section 3.2.

3.1 Modal Displacements

The stiffness matrix $\mathbf{K}$ for small deformation is constant. Thus, we can decouple Eq. (6) by solving the generalized eigenvalue problem $\mathbf{K}\Phi = \mathbf{M}\Phi\Lambda$ and finding the $\mathbf{M}$-orthonormal eigenvectors Φ and the corresponding eigenvalues Λ such that $\Phi^{\mathrm{T}}\mathbf{M}\Phi = \mathbf{I}$ and $\Phi^{\mathrm{T}}\mathbf{K}\Phi = \Lambda$. Since the columns of Φ form a basis of the $6n$-dimensional space, a time-varying generalized displacement vector $\mathbf{u}(t)$ can be expressed as a linear combination of the columns:

$$\mathbf{u}(t) = \Phi\mathbf{q}(t), \tag{7}$$

where Φ is the modal displacement matrix, of which i-th column represents the i-th vibration mode shape of the thin rod, and $\mathbf{q}(t)$ is a vector containing the corresponding modal amplitudes as its components. To reduce the amount of computation significantly, we extract only the m dominant columns of Φ. Hereafter, Φ denotes the $6n \times m$ submatrix composed in this way. By substituting Eq. (7) into Eq. (6) and premultiplying Φ^{T} to both sides, we can make the resulting equations decoupled as follows:

$$\mathbf{M_q}\ddot{\mathbf{q}} + \mathbf{C_q}\dot{\mathbf{q}} + \mathbf{K_q}\mathbf{q} = \Phi^{\mathrm{T}}\mathbf{F}, \tag{8}$$

where $\mathbf{M_q} = \mathbf{I}, \mathbf{C_q} = \xi\mathbf{M_q} + \zeta\mathbf{K_q}, \mathbf{K_q} = \Lambda$ are diagonal matrices so that the m independent equations can be solved individually. The key idea of modal warping techniques is decomposing a large deformation into a series of small deformations to which the above decoupling can be applied; The details will be presented in Section 3.3.

3.2 Modal Rotations

To develop a modal warping technique for thin rods, we should be able to represent the rotational component of deformation in terms of $\mathbf{q}(t)$. More precisely, we need an equation of a form similar to Eq. (7), but this time for $\mathbf{w}(t)$, the $3n$-dimensional composite vector formed by concatenating all the 3D rotation vectors of the mesh nodes.

In the case of 3D solids, the curl $\frac{1}{2}(\nabla \times \mathbf{u})$ gives the rotational component of deformation [16]. However, the curl-based rotation capturing is not applicable to a rod because the differentiation involved in the curl operation should not be done over free 3D space but be restricted to the 1D domain occupied by the rod. In the case of modal warping for shells [17], the rotation $\mathbf{w}(t)$ of a triangle undergoing small deformation is represented in terms of $\mathbf{u}(t)$ through the first-order Taylor expansion, and then it is further expanded in terms of $\mathbf{q}(t)$ using the modal displacement matrix. However, this approach cannot be applied to a rod element, because it can twist freely.

The $6n$-dimensional generalized displacement vector $\mathbf{u}(t)$ is a concatenation of 6 DOFs of

every mesh node, which consists of a positional displacement $\mathbf{u}_i$ and a rotational displacement $\mathbf{r}_i$, as depicted in Fig. 2. By noting this, we can obtain the modal rotation of a thin rod in a straightforward way compared to the cases of a solid and shell, where the modal rotations are computed by averaging the rotational displacements of the elements sharing a node [16, 17]. In the case of a thin rod, however, the rotation vector of each mesh node undergoing infinitesimal deformation is already given in $\mathbf{u}$ (t) as a rotational displacement. Thus, we can obtain the modal rotation vector $\mathbf{w}(t)$ by simply multiplying the $3n \times m$ matrix Ψ, which consists of every even-numbered row of the modal displacement matrix Φ as illustrated in Fig. 2, to $\mathbf{q}(t)$:

$$\mathbf{w}(t) = \Psi \mathbf{q}(t). \tag{9}$$

Φ is characterized by the thin rod at the undeformed state. Thus Ψ is also constant over time, and it can be precomputed. The above equation shows that, as in the generalized displacement in Eq. (7), the local rotations of the mesh nodes can be represented in terms of the modal amplitudes $\mathbf{q}(t)$. We call Ψ the modal rotation matrix.

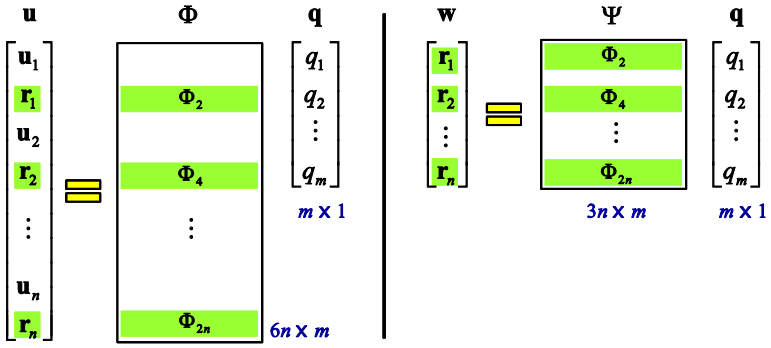

Fig. 2. Finding the rotational component of deformation

3.3 Integration of Rotations

Eq. (9) provides an efficient way of tracking the local rotations occurring at the mesh nodes. However, such rotations are not yet reflected in the computation of the displacement $\mathbf{u}(t)$. Moreover, the results derived in Sections 3.1 and 3.2 hold only when the rotational deformation is moderately small. Both of these problems can be resolved by introducing a local coordinate frame for each mesh node.

We embed a local coordinate frame at each node such that at the rest state it is aligned with the global coordinate frame. In orther words, all the roational displacements $\mathbf{r}_i$'s are simply zeros at the rest state. Let $\mathbf{R}_i(t)$ be the rotation matrix for the local coordinate frame attached to the i-th node at time t, and $\dot{\mathbf{u}}_i^L(t)dt$ be its differential displacement in position measured from its local coordinate frame. Then, the finite positional displacement $\mathbf{u}_i(t)$ measured from the global coordinate frame can be computed as follows:

$$\mathbf{u}_i(t) = \int_0^t \mathbf{R}_i(\tau)\dot{\mathbf{u}}_i^L(\tau)d\tau. \tag{10}$$

The above time integration should be carried out for every node and it can be done in the same way detailed in [16].

To compute Eq. (10) for the finite displacement, we need to obtain $\mathbf{u}^L$, the generalized displacement vector measured in the time-varying local coordinate frames. Eq. (6) is for the infinitesimal deformation. Thus, by premultiplying $\mathbf{R}$ to both sides of Eq. (6) and making assumptions as in [16], we can obtain a new governing equation for $\mathbf{u}^L$:

$$\mathbf{M}\ddot{\mathbf{u}}^L + \mathbf{C}\dot{\mathbf{u}}^L + \mathbf{K}\mathbf{u}^L = \mathbf{R}^{\mathrm{T}}\mathbf{F}, \tag{11}$$

where $\mathbf{R}$ is a 3×3 block diagonal matrix consisting of $\mathbf{R}_i$'s each of which is obtained by simply converting $\mathbf{r}_i$ into the rotation matrix [16].
Finally, we note that (1) the time-varying rotations at the mesh nodes are reflected in Eq. (10), and (2) since it integrates small rotations, the equations derived in Sections 3.1 and 3.2 are now applicable so as to simulate large rotational deformation of a thin rod.

4. Experimental Results

The proposed technique was implemented as an Autodesk MAYA plug-in that runs in a Microsoft Windows 7 Ultimate x64 environment. All experiments described in this section were performed on a PC with an Intel i7 2.93GHz processor, 8GB memory, and an NVIDIA GeForce GT120 graphics card. We fixed the time step size to h = 1/30 seconds but we did not encounter any instability problem.

4.1 Serial Structure

We first conducted an experiment demonstrating the proposed method can simulate large rotational deformation of a thin rod realistically. We applied gravities of different magnitudes to a 20cm long straight thin rod of 4mm radius with rubber-like characteristics: 1,100kg/m^3 density, 11Mpa Young's modulus, and 0.5 Poisson ratio. The simulation mesh has 31 rod elements serially connected by 32 nodes, and the polygonal mesh for surface visualization has 642 vertices, 1,300 edges, and 660 rectangles. **Fig. 3** shows the simulation results applied with gravities of three different magnitudes, 4.9m/s^2, 9.8m/s^2, and 19.6m/s^2. Large rotational deformation was successfully modeled although the simulation was done only with 8 deformation modes.

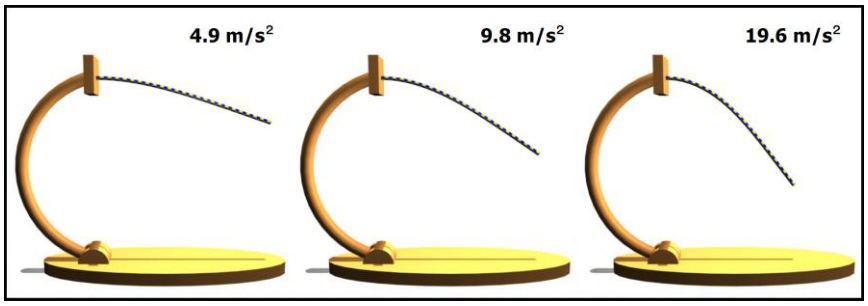

Fig. 3. Thin rods under gravities of different magnitudes

The proposed method need not take any special considerations to simulate a thin rod with an arbitrary rest state. **Fig. 4** shows snapshots of simulating a 51cm long helical thin rod of 8mm radius with 8 deformation modes. The helical rod has the same rubber-like material characteristics with the straight rod in the previous experiment. The simulation mesh has 63

rod elements serially connected by 64 nodes, and the polygonal mesh for visualization has 3,048 vertices, 6,084 edges, and 3,038 rectangles. To generate more dynamic deformation, we attached one end of the helical rod to a sphere keyframed to freely rotate. A rigid rod with the same initial state was also attached to the sphere and then augmented to the snapshots in the transparent yellow color for comparison.

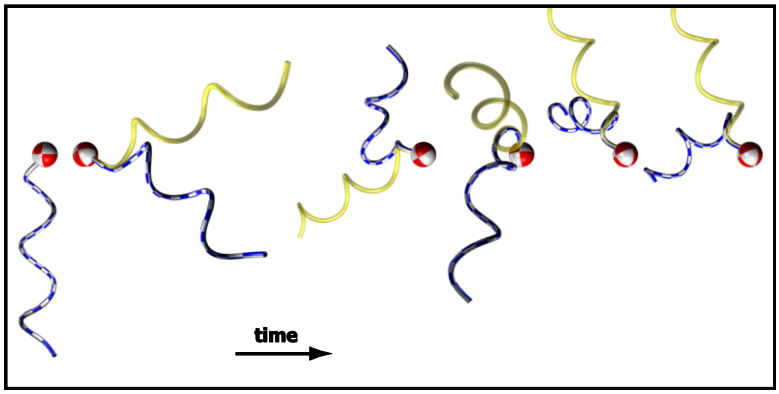

Fig. 4. A rod with a helical rest state

4.2 Cross Sectional Stiffness

Rods with different types of cross sections exhibit different structural stiffness characteristics. Provided with the same area of cross sections, for example, a square-shaped rod is stiffer than a disc-shaped rod, but less stiff than an H-shaped rod. This is because different cross sections result in different area and polar moments of inertia in Eq. (2). **Fig. 5** shows the simulation results obtained with three different types of cross sections. The three rods have the same area of cross sections, densities, Young's moduli, and shear moduli. The disc-shaped rod in the red color is bent the most, the square-shaped rod in the green color the second, and the H-shaped rod in the blue color the least.

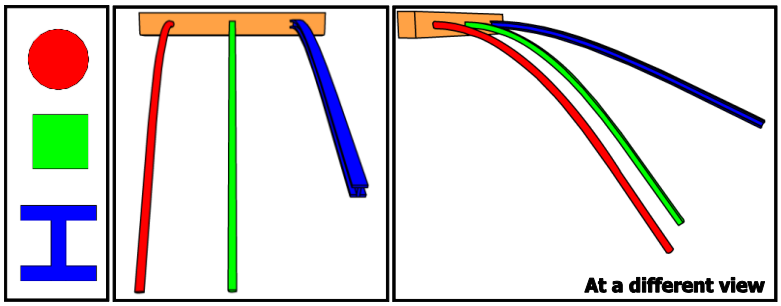

Fig. 5. Simulation of thin rods with different cross sections under the gravity field

4.3 Composite Structure

The proposed technique is applicable to a composite structure with an arbitrary topology. It can simulate not only an open-loop structure represented with a serial chain or with a tree but also a closed-loop structure. **Fig. 6** shows the simulation result of a composite deformable structure connected by many thin rods of 4mm radius. The width and height of the composite structure are 2cm each, and its length is 20cm. The material characteristics are the same with the rubber-like ones in the straight rod example in **Fig. 3** except the density; The density is set to 100 times higher to produce large rotational deformation. The simulation mesh consists of

170 nodes and 336 elements and its corresponding polygonal mesh consists of 7,510 vertices, 14,866 edges, and 7,036 faces. We simulated the composite structure with 8 deformation modes.

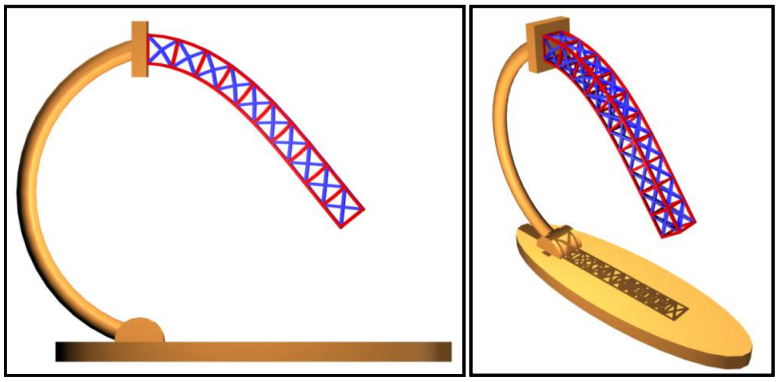

Fig. 6. Deformation of a composite thin rod structure

4.4 Large Mesh

Our method can simulate deformation of a very large mesh in real-time such as a 3D dinosaur-shaped structure in **Fig. 7**. In this experiment, we adopted the dinosaur mesh itself, which consists of 9,836 vertices, 29,502 edges, and 19,668 faces, as a simulation mesh. Each edge is interpreted as a rod element of 8mm radius with the same rubber-like material characteristics. The head of the dinosaur is about 1.4m apart from the tail. To achieve real-time performance, we employed a vertex program on a programmable graphics hardware as in the modal warping techniques for solids and shells [16, 17]. The simulation ran at about 300 fps.

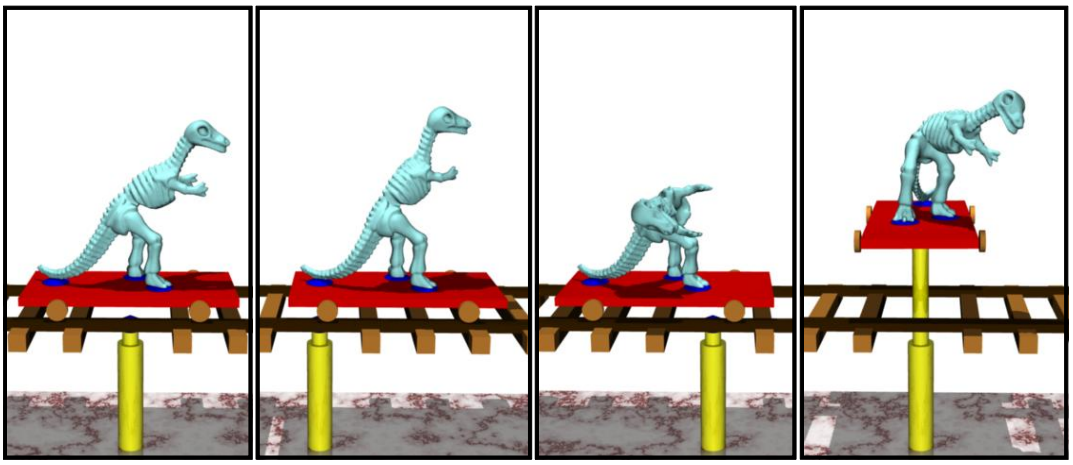

Fig. 7. Real-time deformation of a large mesh

5. Conclusion

In this paper, we proposed a real-time technique for simulating thin rods undergoing large rotational deformation. We formulated the dynamics of a thin rod based on a linear rod theory [10]. Then, we made modifications to the modal warping technique [16], which was originally

proposed for 3D elastic solids, so as to simulate thin rods. The proposed technique ran stably even when the time step size was fixed to $h = 1/30$ seconds, and produced visually convincing results. We expect the proposed technique will prove useful in broad application areas, including computer games and character animation.

The proposed technique is based on the modal warping framework, thus it has the inherent limitations. It adequately accounts for rotational deformation, but it does not preserve the volume strictly. When involved with a large degree of stretching or compression, there might be noticeable artifacts. In addition, even when animating a single undamped mode, the vibration frequency is constant independent of the motion. Such deformations would require nonlinear rod theories. Furthermore, the proposed technique can produce a spurious ghost force when applied to a free-floating deformable object because it is based on node-wise rotation of the stiffness matrix, as noted in [4, 16]. Currently, our work is focused on a thin rod attached to a rigid support, thus the ghost force effects are suppressed by the constraint force acting on a rigid support.

References

[1] J. Barbić and D. L. James, "Real-time subspace integration for St. Venant-Kirchhoff deformable models," *ACM Transactions on Graphics (Proc. ACM SIGGRAPH 2005)*, vol. 24, no. 3, pp. 982–90, 2005. Article (CrossRef Link).

[2] S. Gibson and B. Mirtich, *A survey of deformable modeling in computer graphics*, *Tech. Rep. TR-97-19*, Mitsubishi Electric Research Lab., Cambridge, MA, 1997. Article (CrossRef Link).

[3] D. L. James and K. Fatahalian, "Precomputing interactive dynamic deformable scenes," *ACM Transactions on Graphics (Proc. ACM SIGGRAPH 2003)*, vol. 22, no. 3, pp. 879–87, 2003. Article (CrossRef Link).

[4] M. Müller, J. Dorsey, L. McMillan, R. Jagnow and B. Cutler, "Stable real-time deformations," in *Proc. of ACM SIGGRAPH Symp. Computer Animation 2002*, pp. 49–54, 2002. Article (CrossRef Link).

[5] D. Terzopoulos, J. Platt, A. Barr and K. Fleischer, "Elastically deformable models," *Computer Graphics (Proc. ACM SIGGRAPH '87)*, vol. 21, no. 4, pp. 205–214, 1987. Article (CrossRef Link).

[6] K. Anjyo, Y. Usami and T. Kurihara, "A simple method for extracting the natural beauty of hair," *Computer Graphics (Proc. ACM SIGGRAPH '92)*, vol. 26, no. 2, pp. 111–120, 1992. Article (CrossRef Link).

[7] A. Daldegan, N. M. Thalmann, T. Kurihara and D. Thalmann, "An integrated system for modeling, animating and rendering hair," *Computer Graphics Forum (Proc. EUROGRAPHICS '93)*, vol. 12, no. 3, pp. 211–221, 1993. Article (CrossRef Link).

[8] R. E. Rosenblum, W. E. Carlson and E. Tripp, "Simulating the structure and dynamics of human hair: Modeling, rendering and animation," *The Journal of Visualization and Computer Animation*, vol. 2, no. 4, pp. 141–148, 1991. Article (CrossRef Link).

[9] S. S. Antman, *Nonlinear Problems of Elasticity*, Springer-Verlag, 1995. Article (CrossRef Link).

[10] M. Géradin and D. Rixen, *Mechanical Vibrations: Theory and Application to Structural Dynamics*, John Wiley, 1994. Article (CrossRef Link).

[11] M. B. Rubin, *Cosserat Theories: Shells, Rods and Points*, Kluwer, 2000. Article (CrossRef Link).

[12] D. K. Pai, "STRANDS: Interactive simulation of thin solids using cosserat models," *Computer Graphics Forum (Proc. EUROGRAPHICS 2002)* vol. 21, no. 3, pp. 347–52, 2002. Article (CrossRef Link).

[13] F. Bertails, B. Audoly, M.-P. Cani, B. Querleux, F. Leroy and J.-L. Lévêque, "Super helices for predicting the dynamics of natural hair," *ACM Transactions on Graphics*, vol. 25, no. 3, pp. 1180–1187, 2006. Article (CrossRef Link).

[14] M. Bergou, M. Wardetzky, S. Robinson, B. Audoly and E. Grinspun, "Discrete elastic rods," *ACM*

Transactions on Graphics, vol. 27, no. 3, pp. 63:1–63:12, 2008. Article (CrossRef Link).
[15] M. Bergou, B. Audoly, E. Vouga, M. Wardetzky and E. Grinspun, "Discrete viscous threads," *ACM Transactions on Graphics*, vol. 29, no. 4, pp. 116:1–116:10, 2010. Article (CrossRef Link).
[16] M. G. Choi and H.-S. Ko, "Modal warping: Real-time simulation of large rotational deformation and manipulation," *IEEE Transactions on Visualization and Computer Graphics*, vol. 11, no. 1, pp. 91–101, 2005. Article (CrossRef Link).
[17] M. G. Choi, S. Y. Woo and H.-S. Ko, "Real-time simulation of thin shells," *Computer Graphics Forum (Proc. EUROGRAPHICS 2007)*, vol. 26, no. 3, pp. 349–354, 2007. Article (CrossRef Link).
[18] J. Stam, "Stochastic dynamics: Simulating the effects of turbulence on flexible structures," *Computer Graphics Forum (Proc. EUROGRAPHICS '97)*, vol. 16, no. 3, pp. 159–164, 1997. Article (CrossRef Link).
[19] J. Chang, D. X. Shepherd and J. J. Zhang, "Cosserat-beam-based dynamic response modeling," *Computer Animation and Virtual Worlds*, vol. 18, no. 45, pp. 429–436, 2007. Article (CrossRef Link).
[20] J. Diener, M. Rodriguez, L. Baboud and L. Reveret, "Wind projection basis for real-time animation of trees," *Computer Graphics Forum (Proc. EUROGRAPHICS 2009)*, vol. 28, no. 2, pp. 533–540, 2009. Article (CrossRef Link).

Min Gyu Choi is an associate professor in the Department of Computer Science at Kwangwoon University, Korea. He has been working at Kwangwoon University since 2005. His primary research interests are physics-based modeling and simulation, game physics, and character animation. He received his BS, MS, and PhD degrees in computer science from Korea Advanced Institute of Science and Technology (KAIST), Korea, in 1996, 1998, and 2003, respectively. He was a postdoctoral fellow in the School of Electrical Engineering and Computer Science at Seoul National University, Korea from 2003 to 2005.

Oh-young Song is an associate professor in the Department of Digital Contents at Sejong University, Korea. He has been working at Sejong University since 2006. His primary research interests are physics-based animation and character animation. He received the BS, MS, and PhD degrees in the School of Electrical Engineering and Computer Science from Seoul National University, Korea, in 1998, 2000, and 2004, respectively. He was a postdoctoral fellow in the School of Electrical Engineering and Computer Science at Seoul National University, Korea from 2004 to 2006.